Radiological Impact Assessment of a Prolonged Release from a Pyroprocessing Facility

Robby Christian [a], Hyun Gook Kang [b*]
[a,b]*KAIST, Nuclear & Quantum Eng. Dept., 291 Daehak-ro, Yuseong-gu, Daejeon 305-701*
[*]*Corresponding author: hyungook@kaist.ac.kr*

1. Introduction

Korea Atomic Energy Research Institute (KAERI) has been developing a pyroprocessing technology to process nuclear spent fuels. A demonstration facility termed PRIDE (PyRoprocess Integrated inactive DEmonstration facility) has been built to study and prepare for the construction of the active facility. Prior to that, a radiological impact assessment must be conducted to establish a safe and secure facility design.

Research have been done to identify possible accident scenarios and their impact thereof to the surrounding environment [1,2,3]. However these studies were based on the assumption of a short term release period and a constant meteorological conditions. There has yet a study which examines the environmental impact from a prolonged release of radioactivity from a pyroprocessing facility.

This paper attempts to close the gap by analyzing a certain prolonged release scenario and its radiological consequences.

2. Methods

2.1. Dispersal Model

In the case of environmental impact analysis from a short-term release scenario, several subsequent assumptions are established, i.e., a constant meteorological condition, a straight line plume trajectory, and a relatively limited geographical impact area to be assessed. Therefore a relatively simple Gaussian plume based atmospheric dispersion model may be employed to estimate the spread of radioactive concentration to the environment. In this model shown in Fig. 1, the transport of radioactive material in the downwind direction is governed by a straight-line advection process while the transport in the crosswind and vertical direction is done through diffusion.

This aforementioned approach is not applicable when an extended release period occurs. With longer release periods, there exists a lower likelihood of having a time-invariant meteorological condition around the release point. Furthermore when the geographical region of interest is shaped by prominent wind-altering landscape features such as a river, hill, or valley, the simple plume dispersion model cannot be applied. In addition, it is also desirable to take into account the stochastic effect of turbulence as this effect becomes more significant in affecting the spread of radioactive material when the assessment time is extended.

To estimate the impact from a prolonged release, a dynamic trajectory dispersion model was used. It is a dispersion model on the combination of Eulerian and Lagrangian approach. The Lagrangian approach was used to model the advection and diffusion process, while the Eulerian approach was used to estimate the distribution of concentrations. The HYSPLIT (Hybrid Single-Particle Lagrangian Integrated Trajectory) code provided by the U.S. Department of Commerce, National Oceanic Atmospheric Administration (NOAA) combines these two approaches and was accordingly selected for this analysis.

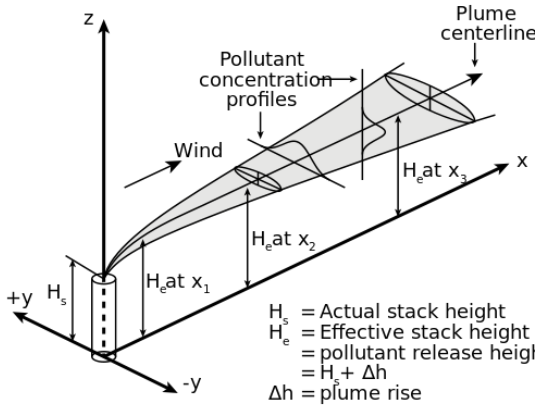

Fig. 1. A Gaussian plume dispersal model

In this current approach, the pollutant dispersal was modeled as both quantized particles and puffs as a tradeoff between simulation accuracy and computational time. The vertical transport was modeled with the particles approach, while the horizontal transport was approximated as puffs having an isotropic Gaussian diffusion with a Lagrangian centerline trajectory as shown in Fig 2. As pollutant's concentration is dissolved, the puff's size continue to grow until it exceeds the meteorological grid dimension. Beyond this critical size the puff may split into smaller puffs, each with its own proportion of pollutants concentration. The different puffs are transported with independent trajectories and may be carried away from each other or may merge again as a single puff when they are in the same coordinate.

As the Eulerian model relies on the discretization of spatial dimension to solve the pollutant's concentration differential equation, a grid of meteorological data is required in this model. In this study, the grid from the Global Data Analysis System (GDAS) was used. It has a sufficient resolution of 0.5 degrees and a global coverage. The data is maintained and updated daily by the NOAA and can be accessed online.

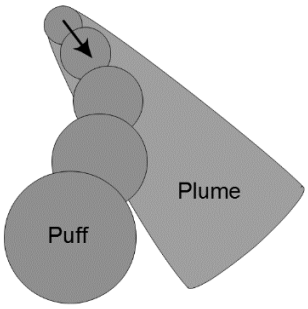

Fig 2. Illustration of Gaussian puff and plume

2.2. Release Scenario and Source Term Estimation

The engineering scale pyroprocessing facility designed by KAERI uses the 16x16 PWR type spent fuel as the reference spent fuel. It has a 4.5wt% U-235 enrichment with a 55,000 MWD/MTU burnup and 10 years cooling period. The maximum throughput is 10 tHM per year. With this data, the base radioactive material inventory was calculated using the ORIGEN-ARP code by taking the PLUS7 fuel design as the reference.

Referring to the pyroprocessing process flow diagram shown in Fig 3, Moon et. al. considered the release of radioactive material from the hot cell as the greatest accident event influencing exposure at the site boundary [2]. This is due to the fact that it involves the damage of off-gas treatment system which is designed to trap fission products and protect against the release of nuclides into the environment [4]. The source term involved in the accident was then calculated from the base radioactive material under the following conditions and assumptions:

(1) The nuclides removal ratio from the head-end process to the off-gas treatment follows the facility's technical specification.
- Kr/Xe: 100%
- Cs: 98%
- I: 100%
- Tc: 92.3%
- Ru: 97.6%
- Te: 53.3%
- Rb: 96%

(2) Release fraction values were taken from the US-DOE publication for a Hazard Category 2 facility [5].
- Kr/Xe: 100%
- Cs: 1%
- I: 50%
- Tc: 0.1%
- Ru: 1%
- Te: 1%
- Rb: 0.1%

(3) Continuous release of the whole inventory over a period of 12 hours.

The site location was assumed to be at KAERI. Two distinct time windows were selected to evaluate the effect of dispersal. The selection was done in regard to the contrasting ratio of daytime to nighttime hours which in turn affects the change of atmospheric conditions during the release period. One period was chosen to be during the solstice and another was during the equinox.

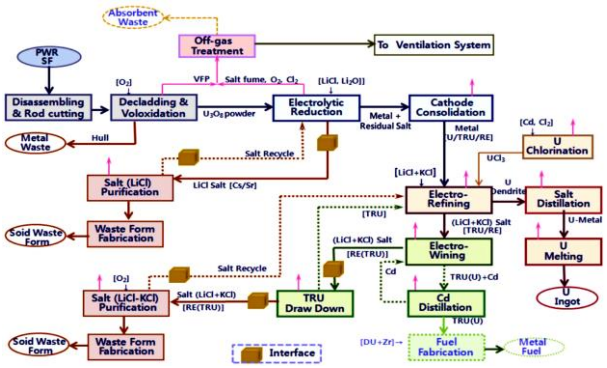

Fig. 3. Process Flow Diagram of Pyroprocessing

2.3. Uncertainties

Cox stated that small errors in inputs to an atmospheric model will be amplified and doubled every five days [6]. This significantly contributes to the uncertainty of final results obtained from an atmospheric dispersion model. Therefore in order to manage the uncertainties arising from variations in input variables, an ensemble system was utilized. The schematic of this system is given in Fig. 4. It works by creating different individual models which give different outcomes and combines them to form an aggregated outcome.

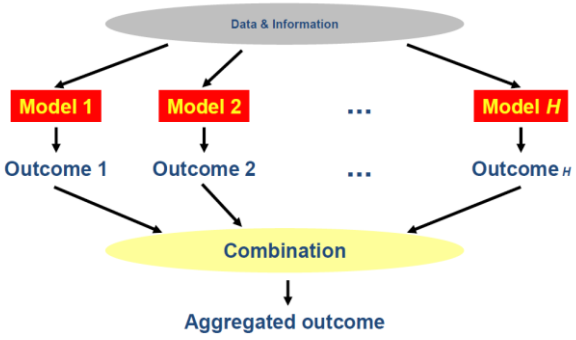

Fig. 4. Ensemble System

The inputs to the model in this study are comprised of both deterministic wind map and stochastic turbulence factors. Consequently, variations to these input variables served as the basis of diversifying the models in the ensemble system. It was expected that the true state of outcome falls within the predicted ensemble spread. For the creation of ensemble from the deterministic input variable, first consider that the source location lies at a certain point within a three dimensional meteorological grid cell as shown in Fig. 5. Horizontal offsets in the X

and Z axis and a vertical offset in the Y axis were chosen. Random isotropic samples between the source location and the offsets were then extracted. The sampled locations were then used to translate the meteorological grid data to the source's location while keeping the source's location itself constant. For the ensemble from the stochastic input, the models were initiated with different random number seeds. The ratio between the number of models which are in agreement with an output and the total number of models constitutes as the probability value for the respective output.

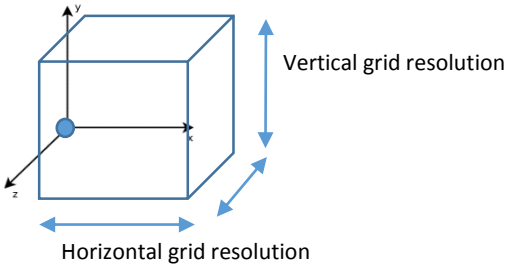

Fig. 5. Point source within a grid cell

2.4 Dose Conversion Factors (DCFs)

The Federal Guidance Report (FGR) 13 was chosen as the dose conversion factor. With this option, the human lung was modeled based on the International Commission on Radiation Protection (ICRP) Publication 66 while dose coefficients were taken from ICRP Publication 60. The reference man was assumed to have a breathing height of 1.5 meter and a breathing rate of 3.47E-4 m^3/s.

The HYSPLIT code estimates the distribution of radioactive material concentration. The conversion from concentration to radiological dose was therefore done in the post-processing phase [7]. The dose was then compared to the dose limits regulated in the Notice of the NSSC No. 2012-03.

3. Results and Discussions

Several important variables of the 2014 solstice meteorological data windowed around the Korean peninsula is shown in Fig 6. From the upper left in a clockwise manner, it shows the hourly wind direction, precipitation rate averaged over 6 hour periods, hourly vertical wind velocity, and hourly horizontal wind velocity the surface height level at 00:00 GMT 21 June 2014. Meanwhile, the same variables for the 2014 equinox is shown in Fig 7. The white color for precipitation and wind speed indicates that the value is out of the preset scale.

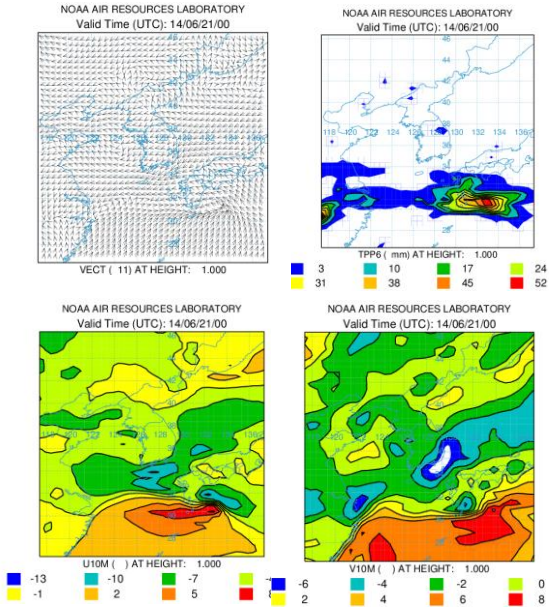

Fig 6. 2014 Solstice meteorological data

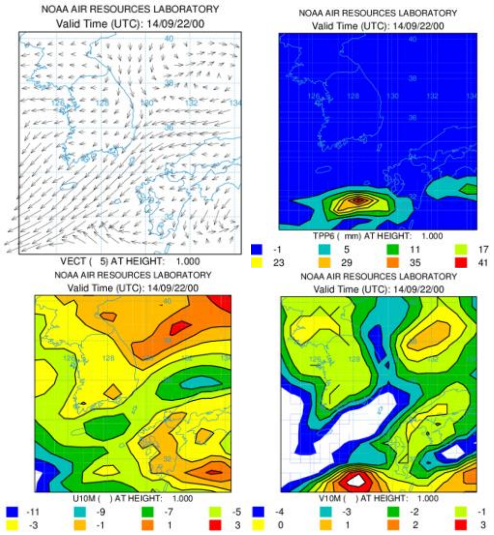

Fig 7. 2014 Equinox meteorological data

The resulting pollutant's transport trajectories and altitude for the 2014 solstice and equinox are given in Fig 8 and Fig 9 respectively. The end of trajectories were not defined by the threshold of pollutant's concentration but rather by the limit of simulation time. Fig 8 shows the influence of sea breeze in diverting the path of radioactive puffs back into the peninsula. This is because in June during daytime the temperature gradient between the sea and the land creates a surface wind coming to the land. A contrasting phenomenon occurs during equinox, which is shown in Fig 9. This result would not be observed if the Gaussian plume dispersal model had been used. The vertical trajectory profile was consistent with the terrain structure around the trajectory.

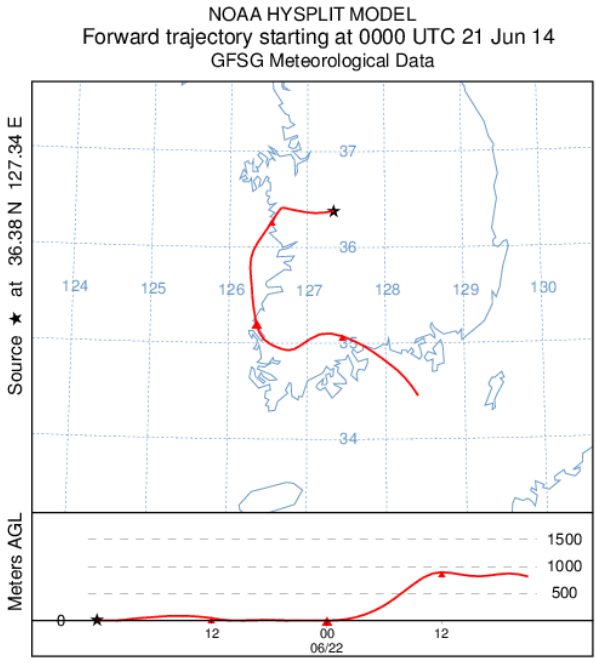

Fig 8. Pollutant's trajectory during solstice

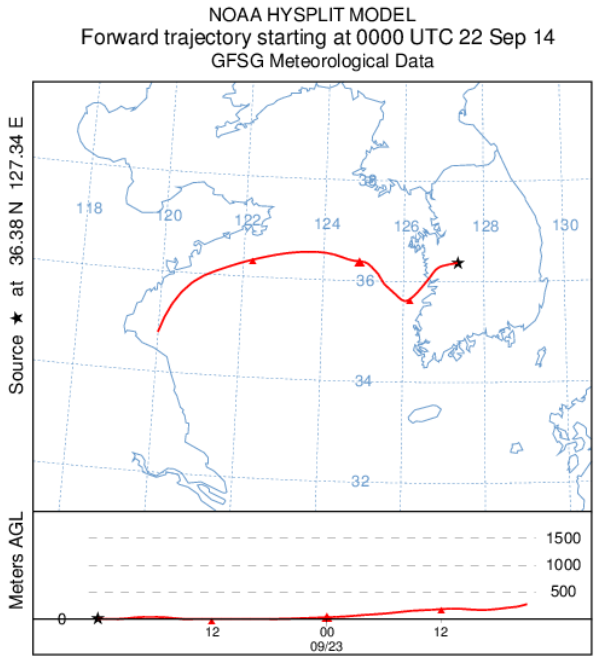

Fig 9. Pollutant's trajectory during equinox

Fig 10 shows the averaged values of radioactive material concentration during solstice. The concentration unit is not expressed in physical quantities but rather in computational quantity, number of particles/m^3. These values represent both the particulates and gaseous form of the emitted source term. The relatively low values of concentration agrees to the classification of a pyroprocessing facility which falls into a Hazard Category 2 facility [5]. Facilities in this category are less likely to cause significant off-site consequences. Instantaneous profile of puffs were recorded and stacked together as shown in Fig 11 to give information regarding their time of arrival. Converting the concentration values to radiological dose confirms this statement, as seen in Fig 12. The maximum observed dose was 26 mR near the release site, which resulted from integrating the dose over a period of two days.

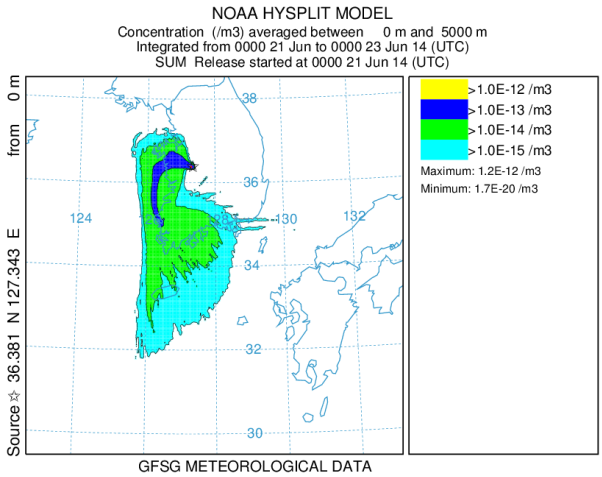

Fig 10. Averaged radioactive material concentration in solstice simulation

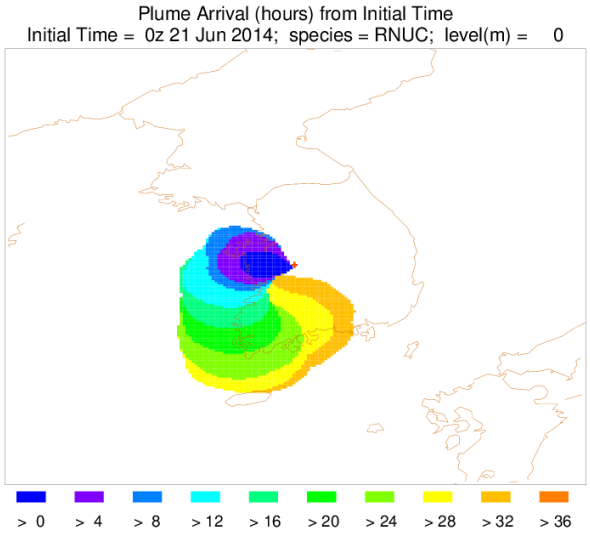

Fig 11. Radioactive material arrival time in solstice simulation

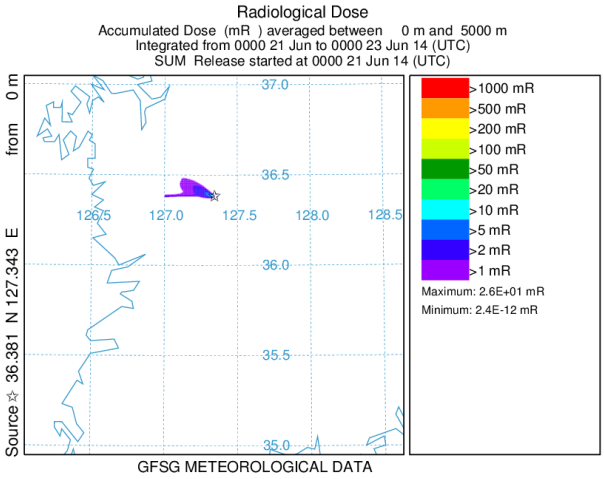

Fig 12. Radiological dose in solstice simulation

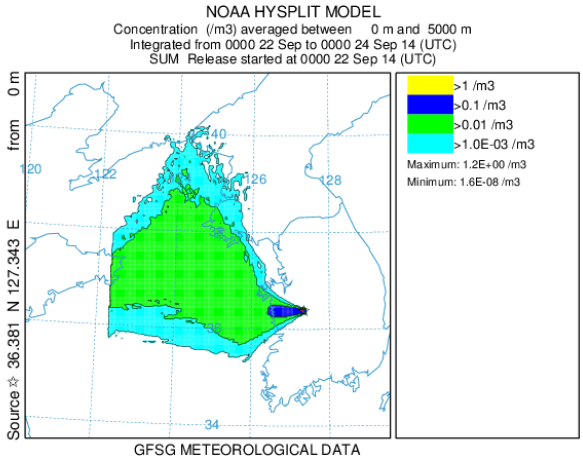

Fig 13. Averaged radioactive material concentration in equinox simulation

The averaged profile of radioactive material concentration during September 2014 equinox is given in Fig 13. It shows that the radioactive material was carried out towards the sea. The cutoff shown at the left hand side of the profile was caused by the windowing of the assessment region which was set to 5 degrees from the emission site. This window was deemed sufficient to cover the Korean peninsula and the surrounding areas. The limitation was made to reduce computation time. Fig 14 shows the arrival time of the radioactive materials, while Fig 15 shows the cumulative radiation dose profile. As expected, the resulting radiation dose was relatively low. However there was an area near the site where the dose is above 1 Rem. This might be caused by the rounding effect from the meteorological grid. In the equinox simulation, a coarser grid resolution was used to reduce computation time since the concentration spread was larger than the solstice simulation. Moreover, the concentration distribution near site in general is more affected by deterministic turbulence caused by structures and buildings-wake effect rather than a stochastic one as studied in this paper. A study based on the computational fluid dynamics is expected to give a better prediction on the concentration and dose distribution near the plant site. A more precise data on arrival times may be acquired by monitoring the cities around the emission site. Four neighboring cities were selected for this purpose, and the puff's arrival times are shown in Fig 16. The records were consistent with the averaged profile shown in Fig 14 and Fig 17.

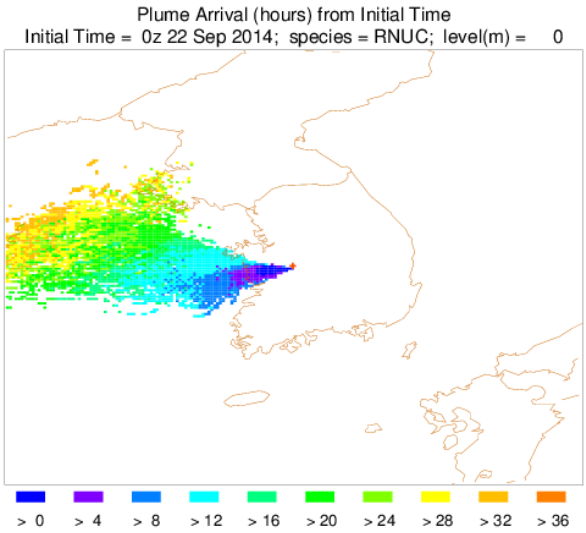

Fig 14. Radioactive material arrival time in equinox simulation

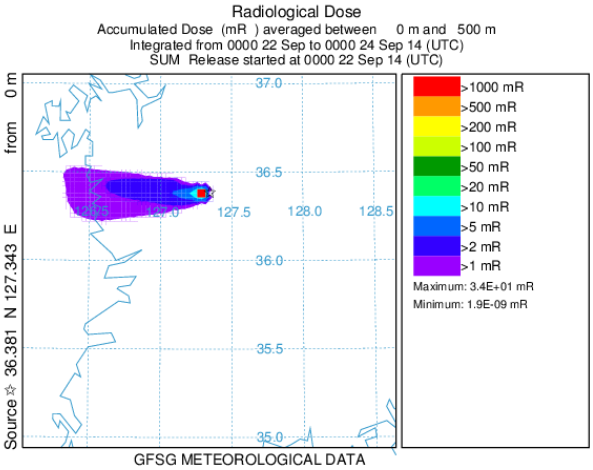

Fig 15. Radiological dose in equinox simulation

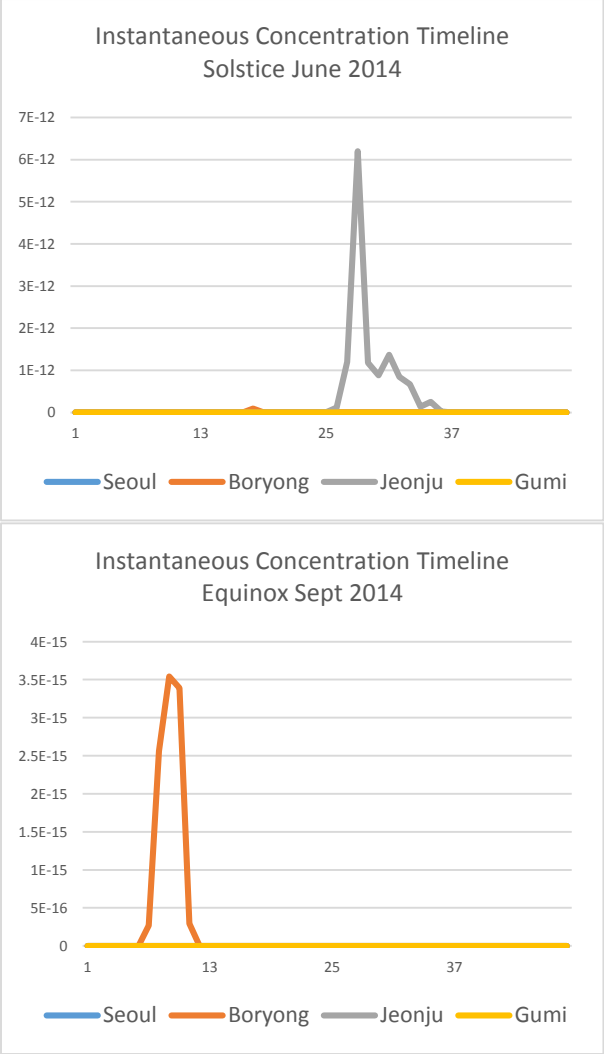

Figure 16. Instantaneous radioactive concentration and arrival time in major cities around the release site during solstice (top) and during equinox (bottom)

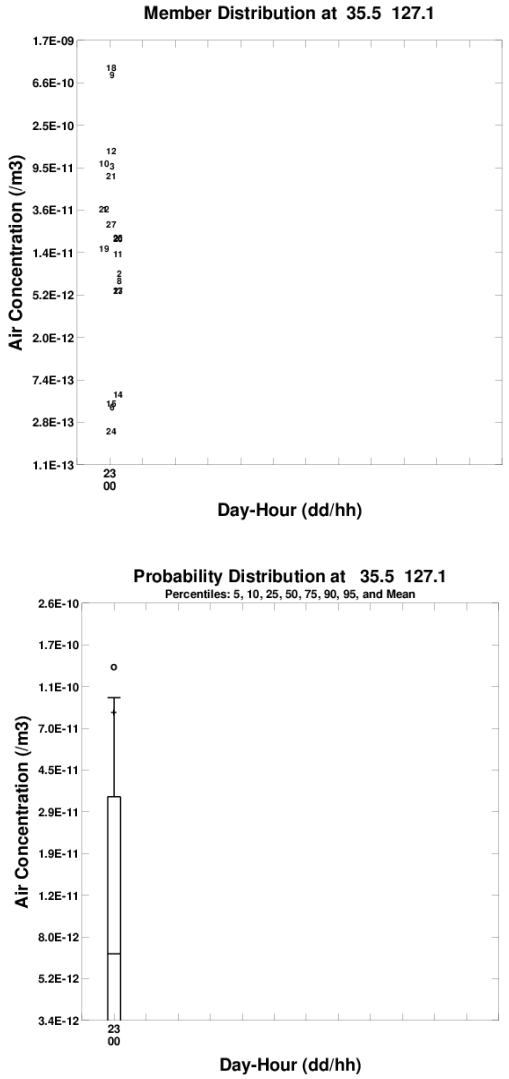

Figure 17. Radioactive concentrations at Jeonju city from the deterministic ensemble (top) and the statistical representation in a box-plot (bottom)

Results for the deterministic ensemble are shown in Fig 17, while results for the stochastic ensemble are illustrated in Fig 18. It is observed from the figures that the deterministic ensemble is more sensitive to determining the final concentration compared to the stochastic ensemble. The box plots of these ensembles give probability distributions of the concentrations. It is important to note however that in order to take into account both deterministic and stochastic uncertainties, a grand ensemble might be required. However as an ensemble's size grows, the computational time grows exponentially. Therefore in the coming work, an approach to an ensemble feature selection and reduction based on their importance and sensitivity will be investigated. Moreover, the optimal parallelization of an ensemble to further reduce computational time will be studied.

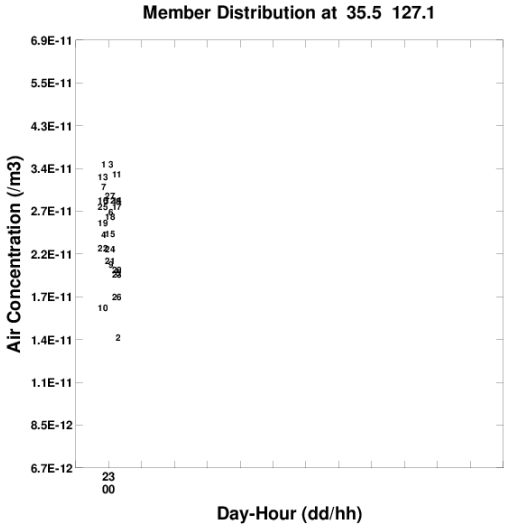

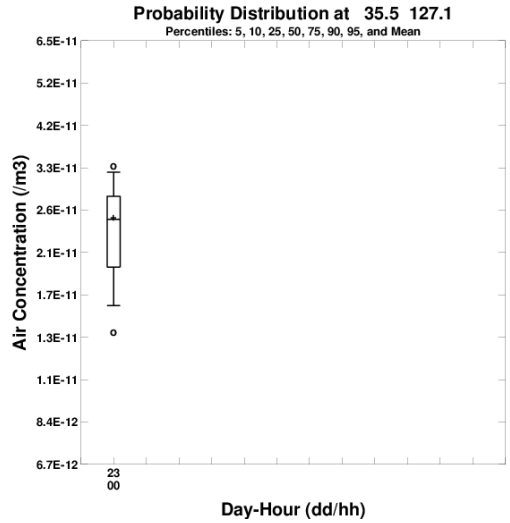

Figure 18. Radioactive concentrations at Jeonju city from the stochastic ensemble (top) and the statistical representation in a box-plot (bottom)

4. Conclusions

The results showed an agreement with the previous research which concluded that the radiological impact to the surrounding environment of a pyroprocessing facility is below the prescribed regulatory limits. Furthermore this study showed that the transport path might be dynamic enough to reflect escaping puffs back to the geographical region of interest. It also showed the prominent effect of the wind vector and velocity changes at the source release point to the final distribution of radioactive material concentration. An effect which should not be neglected particularly in a prolonged release period scenario.

Ensemble systems were able to manage uncertainties from meteorological data and random turbulence simulations. The accuracy of meteorological data was more sensitive to the aggregated concentration distribution compared to the differences in random turbulence simulations. Further work might be extended to include ensembles of the modelling process and/or their parameters such as puff splitting and merging, precipitation rate, and the occurrence of inversion layers in the atmosphere.

REFERENCES

[1] G.S. You, I.J. Cho, W.M. Choung, E.P. Lee, D.H. Hong, W.K. Lee, and J.H. Ku, Concept and Safety Studies of an Integrated Pyroprocess Facility, Nuclear Engineering and Design Vol. 241, pp. 415-424

[2] S.I. Moon, W.M. Chong, G.L. You, J.H. Ku, H.D. Kim, Y.K. Lim, and H.S. Chang, Preliminary Safety Study of Engineering Scale Pyroprocess Facility, Nuclear Engineering and Technology Vol. 46, pp. 63-72

[3] R. Christian, H.G. Kang, Radiological Impact Assessment on a Sabotage of Spent Fuel Handling in a Pyroprocessing Facility, Proceeding of Korean Nuclear Society Autumn Conference, 2014.

[4] H. Lee, G.I.Park, K.H. Kang, J.M. Hur, J.G. Kim, D.H. Ahn, Y.Z. Cho, E.H. Kim, Pyroprocessing Technology Development at KAERI, Nuclear Engineering and Technology Vol. 43 Issue 4 pp. 317-328, 2011.

[5] U.S. Department of Energy, Hazard categorization and accident analysis techniques for compliance with DOE order 5480.23, Nuclear safety analysis reports, DOE-STD-1027-92, 1992.

[6] J.D. Cox, Storm Watchers: The Turbulent History of Weather Prediction from Franklin's Kite to El Nino, ISBN 0-471-38108-X, 2002

[7] U.S. National Oceanic and Atmospheric Administration, Handbook on Atmosperic Dispersion, Prepared for the U.S. Department of Energy, DOE/TIC-11223, 1982